AD-A115 648 FOREIGN TECHNOLOGY DIV WRIGHT-PATTERSON AFB OH F/G 20/5
WAVEGUIDE GAS LASER,(U)
MAY 82 C ZEDONG
UNCLASSIFIED FTD-ID(RS)T-0356-82 NL

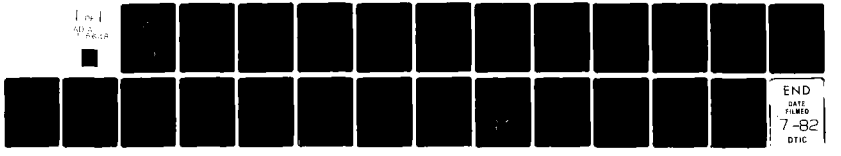

END
DATE FILMED
7-82
DTIC

AD A115648

FTD-ID(RS)T-0356-82

FOREIGN TECHNOLOGY DIVISION

WAVEGUIDE GAS LASER

by

Cheng Zedong

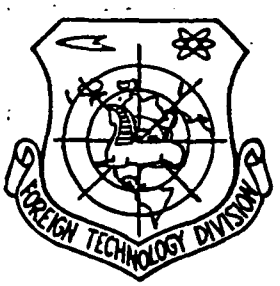

DTIC
ELECTE
JUN 16 1982
S
A

Approved for public release;
distribution unlimited.

DTIC FILE COPY

82 06 16 115

GRAPHICS DISCLAIMER

All figures, graphics, tables, equations, etc. merged into this translation were extracted from the best quality copy available.

EDITED TRANSLATION

FTD-ID(RS)T-0356-82 26 May 1982

MICROFICHE NR: FTD-82-C-000686

WAVEGUIDE GAS LASER

By: Cheng Zedong

English pages: 21

Source: Wuli, Vol. 10, Nr. 6, June 1981, pp. 337-344

Country of origin: China
Translated by: LEO KANNER ASSOCIATES
F33657-81-D-0264
Requester: FTD/TQTD
Approved for public release; distribution unlimited.

THIS TRANSLATION IS A RENDITION OF THE ORIGINAL FOREIGN TEXT WITHOUT ANY ANALYTICAL OR EDITORIAL COMMENT. STATEMENTS OR THEORIES ADVOCATED OR IMPLIED ARE THOSE OF THE SOURCE AND DO NOT NECESSARILY REFLECT THE POSITION OR OPINION OF THE FOREIGN TECHNOLOGY DIVISION.

PREPARED BY:

TRANSLATION DIVISION
FOREIGN TECHNOLOGY DIVISION
WP-AFB, OHIO.

WAVEGUIDE GAS LASER

Cheng Zedong
Chengdu College of Telecommunications Engineering

I. General Descriptions

Since the completion of the waveguide He-Ne laser in 1971 by P. W. Smith [1] of the Bell Laboratories, considerable development [2-5] has been done on the waveguide gas laser, especially the waveguide CO_2 laser with very wide range of frequency modulation. The waveguide CO_2 laser is very useful in laser communications, laser radar, laser spectrum, and contamination examination and measurement.

Figure 1 shows the principle of ordinary and waveguide lasers. In an ordinary laser, light propagates between two reflective mirrors according to the propagation law of free space while in the waveguide laser, light propagates in the waveguide, which occupies only a part of the space between two reflective mirrors. Therefore, the theory of the resonance oscillation cavity of the ordinary laser is not applicable to the waveguide laser.

The working media of the waveguide laser include gases, liquids, solids and semiconductors. Hollow tube waveguides should be used for gas and liquid waveguide

lasers, while solid waveguides are used in solid and semiconductor waveguide lasers. The material used for the waveguide may be a medium or a metal. The waveguide gas laser with adoption of discharge excitation should use a hollow tube metal waveguide. Among waveguide gas lasers, the hollow-tube light waveguide is also a discharge capillary; therefore, the waveguide guides light waves and contains discharge gas.

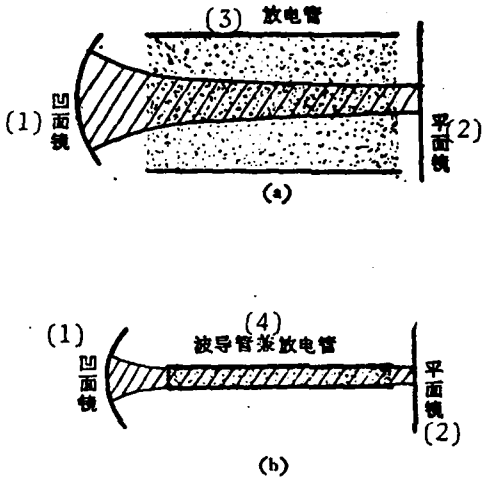

Fig. 1. Principles of waveguide and ordinary lasers: (a) Ordinary gas laser; (b) Waveguide gas laser. Key: (1) Concave mirror; (2) Plain mirror; (3) Discharge tube; (4) Waveguide tube used as discharge tube.

Accession For
NTIS GRA&I
DTIC TAB
Unannounced
Justification
By
Distribution/
Availability Codes
Dist
A-1
DTIC
COPY
INSPECTED
2

One of the most fundamental structural characteristics of the waveguide gas laser is the very small aperture diameter of the discharge tube. For example, in an ordinary CO_2 laser, the inner diameter of the discharge tube is approximately 5 to 15 mm, while the aperture diameter of the discharge tube of a waveguide CO_2 laser is approximately 0.5 to 3 mm [6].

Another fundamental structural characteristic of the waveguide gas laser is that the reflective mirror should be properly arranged; i.e., the output of the waveguide laser is closely related to the radius of curvature of the reflective mirror and the distance from the reflective mirror to the inlet of the waveguide.

The most important characteristic of the waveguide CO_2 laser is its wide range of frequency modulation; this is due to adopting a very small aperture diameter of the discharge tube, so that the high allowable total gas pressure causes very broad pressure intensity lines in the spectrum.

Another important characteristic of the waveguide gas laser is the good directional stability of its output laser beam. This is because in the waveguide gas laser, stability of the light beam direction is basically determined by stability of the axial line of the waveguide. Unlike with the ordinary gas laser, the stability of light beam direction is determined by the angle stability of the reflective mirror in the resonance oscillation cavity.

Besides, compared with the ordinary gas laser, there are the advantages to the waveguide laser that the requirement of adjustment accuracy of the mirror is relatively low and the operation is relatively stable.

II. Transmission Loss of Hollow Tube Light Waveguide

First, an example is shown in Fig. 2 for a hollow tube waveguide with a circular cross section.

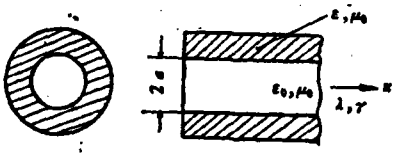

Fig. 2. Hollow tube light waveguide with circular cross section.

According to electromagnetic field theory, there are three modes of light propagation in the hollow tube waveguide: TE [transverse electric] mode, TM [transverse magnetic] mode, and EH [mixed] mode [7]. If we assume

$$\begin{cases} a \gg \lambda, \\ \left|\dfrac{\gamma}{K} - 1\right| \ll 1, \end{cases} \qquad (1)$$

Here, a is the diameter of the waveguide, λ is the wavelength in free space, γ is the propagation constant of light along direction z in a waveguide, and $K = \omega \cdot \sqrt{\varepsilon_0 \mu_0} = 2\pi/\lambda$ is the propagation constant of light in a vacuum. By solving the Maxwell equation and utilizing the boundary conditions at the tube wall, the field component equations of TE_{om}, TM_{om} and EH_{nm} can be obtained. From these equations, distributions of the transverse-direction electric field of these modes with lower orders can be plotted, as shown in Fig. 3 [7].

Table 1. m-th order root of the Bessel function J_{n-1}.

n \ m	1	2	3	4
1	2.405	5.520	8.654	11.796
2 或 0	3.832	7.016	10.173	13.324
3 或 -1	5.136	8.417	11.620	14.796
4 或 -2	6.380	9.761	13.015	16.223

(*)

Key: (*) Or.

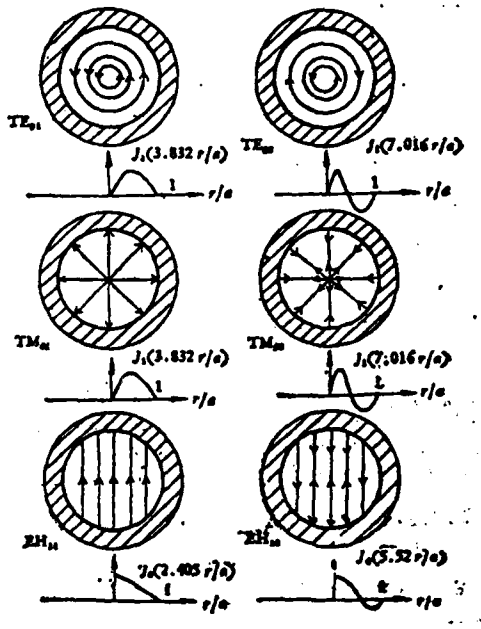

Fig. 3. Hollow tube light waveguide with circular cross section.

Figure 3 shows that the waveguide modes of EH_{1m} category are modes of linear polarization.

The factor $e^{i(\gamma z-\omega t)}$ in the field component equation describes the fact that light propagates along the z direction. The propagation constant $\gamma=\beta_{nm}+i\alpha_{nm}$. Here, β_{nm} is the phase coefficient and α_{nm} is the attenuation coefficient. For an ideal hollow tube straight waveguide, the attenuation coefficient of low-order mode is

$$\alpha_{nm}=\mathrm{Im}[\gamma]=\left(\frac{u_{nm}}{2\pi}\right)^2\frac{\lambda^2}{a^3}\mathrm{Re}(\nu_n), \quad (2)$$

In the equation, u_{nm} is the m-th order root of the Bessel function J_{n-1}; ν_n is related to the material (with refractive index of ν) of the non-metal medium tube wall; and the relationship between ν_n and ν is determined by the type of waveguide mode.

$$\nu_n=\begin{cases}\dfrac{1}{\sqrt{\nu^2-1}}, & TE_{0m}^{(*)}\text{模}\ (n=0),\\ \dfrac{\nu^2}{\sqrt{\nu^2-1}}, & TM_{0m}^{(*)}\text{模}\ (n=0),\\ \dfrac{\nu^2+1}{2\sqrt{\nu^2-1}}, & EH_{nm}^{(*)}\text{模}\ (n=1),\end{cases} \quad (3)$$

Key: (*) Mode.

Under ordinary conditions, the refractive index ν of the material of the waveguide tube wall is a complex number; i.e., $\nu=n-ik$. n and k are determined, respectively, by the dielectric constnat and electric conductivity of the non-metal medium material.

From equations (2) and (3), we obtain the following:

1. $\alpha_{nm}\propto(u_{nm})^2$, values of u_{nm} are listed in Table 1. We can see from the table that (among TE_{om}, TM_{om} and EH_{nm}) TE_{01}, TM_{01} and EH_{11} are the lowest-order modes, which are also the lowest-loss modes. With increasing orders of modes, the attenuation coefficients increase accordingly.

2. $\alpha_{nm}\propto\lambda^2/a^3$, that is, the loss increases rapidly with decreasing aperture diameter of the waveguide.

3. $\alpha_{nm} \propto Re(\nu_n)$, for the case when ν is a real number; in the case of glass $\nu = \sqrt{\varepsilon/\varepsilon_0}$, ε and ε_0 are, respectively, the dielectric constants of the medium and the vacuum. Figure 4 shows curves of varying α_{nm} with ν according to equations (2) and (3). As indicated in the figure, the loss of the TM_{01} mode is the highest in all three lowest-order modes. As for the loss situation of TE_{01} and EH_{11} modes, the losses are determined by the material used for the waveguide (magnitude of ν). When $\nu > 2.02$, the loss of the TE_{01} mode is the lowest. When $\nu < 2.02$, the loss of the EH_{11} mode is the lowest. The most ideal refractive index of the medium for EH_{11} mode transmission should be approximately $\sqrt{3}$.

For example, if boron-silicate glass with $\nu \approx 1.5$ is used as a hollow tube light waveguide, the mode with the lowest loss in transmission is the EH_{11} mode. When $\lambda = 1$ micron and $a = 1$ mm, substitute $u_{11} = 2.405$ in equation (2). It can be calculated that $\alpha_{11} = 0.213 \cdot 10^{-5} cm^{-1}$. Since the transmission loss L_T of a unit length is $e^{\alpha_{11}}$ or expressed in decibels (dB) as

$$L_T = 20 \log e^{\alpha_n} = 8.686 \alpha_n \quad [dB/cm], \qquad (4)$$

For this example, $L_T = 1.85 \cdot 10^{-5}$ dB/cm = 1.85 dB/km.

Here, what we term loss is the so-called "leaking mode" loss [8], which is not related to the loss tangent of the medium and does not include scattering loss because of imperfection in surface. The "leaking mode" loss is caused by the refractive index in the waveguide zone of the hollow tube (non-metal medium) waveguide being smaller than the refractive index outside of the zone. Because according to geometric optics, at that time for light at the inner wall of the waveguide emitted from the inside of waveguide, this is emission from an optically sparse medium to an optically dense medium. Therefore, even the incidence forms a very small grazing angle, and this will not become a total internal reflection. This part of light leaking from the waveguide zone becomes the transmission loss of the hollow tube waveguide discussed above.

When a hollow tube waveguide is not straight, the transmission loss will be higher. Marcatili [7] discussed the situation of the curved waveguide axis line

with a radius R; he obtained

$$\alpha_{nm}(R) = \alpha_{nm}(\infty) + \frac{4}{3}\left(\frac{2\pi}{u_{nm}}\right)^2 \times\left(\frac{a^3}{\lambda^2 R^2}\right)\mathrm{Re}[\nu_n V_{nm}(\nu)], \qquad (5)$$

In the equation, the first item $\alpha_{nm}(\infty)$ is the attenuation coefficient of the hollow tube straight waveguide ($R\to\infty$) given in equation (2); the coefficient is proportional to $u_{nm}^2\lambda^2/a^3$. The second item is the increase of attenuation coefficient caused by the bent axis of the waveguide; the coefficient is proportional to $a^3/\lambda^2 u_{nm}^2 R^2$. In equation (5), $\mathrm{Re}[\nu_n V_{nm}(\nu)]$ is the function of the included angle between the refractive index ν and the polarization direction of the bent surface (of the waveguide axis) and the propagated radiation field. From equation (5), it can be derived that when the attenuation coefficient is doubled (the coefficient in straight waveguide) with twice the bent radius as shown in the following equation,

$$R_0 = \frac{2}{\sqrt{3}}\left(\frac{2\pi}{u_{nm}}\right)^2 \frac{a^3}{\lambda^2}\mathrm{Re}V_{nm}(\nu). \qquad (6)$$

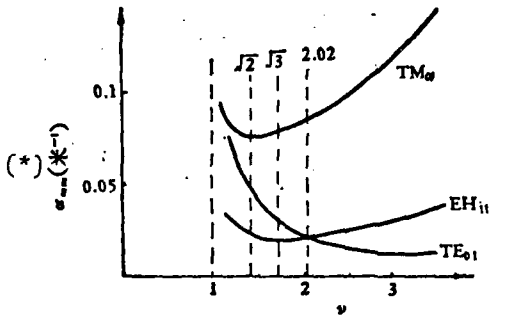

Fig. 4. Relationship between attenuation coefficient and refractive index.
Key: (*) (m^{-1}).

For a hollow tube glass (ν=1.5) waveguide with λ=1 micron and a=1 mm, with the lowest loss EH_{11} mode, α_{11}=1.85 dB/km. The radius of curvature R_o is approximately equal to 10 km with double loss; therefore, the transmission loss of this type of hollow tube light waveguide is quite sensitive to a bent waveguide.

Compared with hollow tube non-metal medium light waveguide, the transmission loss of a hollow tube metal light waveguide is considerably smaller and not so sensitive to the effect of a bent waveguide, because in the light frequency range, the dielectric constant of metal is considerably greater than that of a medium. As shown in Fig. 4, the lowest loss mode is the TE_{01} mode for transmission in a hollow tube metal waveguide; the loss is considerably smaller than the loss in the EH_{11} mode of a hollow tube medium waveguide. By taking aluminum as an example, when λ=1 micron and a=1 mm, the transmission loss of the TE_{01} mode is only 0.028 dB/km. When λ=1 micron and a=0.25 mm, the transmission loss is 1.8 dB/km. At that time, the radius of curvature R_o with doubling loss is approximately 48 meters; that is, the effect on transmission loss by a bent waveguide is relatively small. The reason for decreasing R_o is due to decreasing a in equation (6) and a greater u_{01} (TE_{01} mode) than u_{11} (TE_{01} mode).

The hollow tube metal light waveguide may be useful in the light pump infrared waveguide gas laser because no discharge is required for excitation.

Although there is "leaking mode" loss in the hollow pipe light waveguide, yet only with proper selection of waveguide material and good optical processing on the inner surface of the waveguide, can the transmission loss of the waveguide be considerably smaller than the increment of the laser. This will not affect the operation of the waveguide laser to a great extent.

For the 10.6 micron wave band, ordinary materials, such as BeO, Al_2O_3 and SiO_2 (melted quartz), are materials with losses; that is, the refractive index is a complex number. Abrams [3] calculated $Re(\nu_n)$ by using data in two cases of E//c and E$\perp$c with BeO and Al_2O_3 monocrystal material, as shown in Fig. 5. Abrams considered that the loss of polycrystal material should be a value between these two cases, then he derived the estimated loss values of these non-metal

medium waveguides. For a tube with d=1 mm,

$$\alpha_{11}\begin{cases} 4.3\times10^{-5}\ (\text{cm})^{-1} & (\text{for BeO}), \\ 1.8\times10^{-3}\ (\text{cm})^{-1} & (\text{for } SiO_2). \end{cases}$$

In Fig. 5, losses of Al_2O_3 and SiO_2 are not much different; however, the loss of BeO is less than one-tenth of other materials for transmission through a 10.6-micron-frequency waveguide. Hall [6] conducted experimental measurements on transmission losses of three (medium) materials, BeO, Al_2O_3 and pyrex glass. He proved the proportional relationship between α_{11} and $1/a^3$ and conjectured that loss of BeO is considerably smaller than for other materials. The loss values of glass and Al_2O_3 were measured to be 2 to 3 times greater than that conjectured; this can be explained by the fact that the waveguide used in experiments was not straight and did not have a sufficiently smooth surface, and especially it was not sufficiently clean (foreign micro-particles) inside the waveguide. Hall concluded that if only in the aspect of waveguide loss, for a hollow pipe light waveguide with diameter greater than 1.5 mm, the waveguide can be used, then even the losses for Al_2O_3 and glass are more than 10 times greater than for BeO.

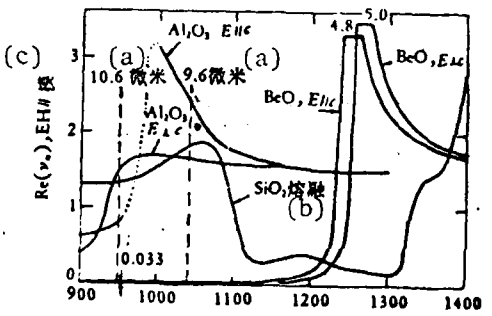

Fig. 5. Relationship between frequency and $Re(\nu_n)$ of BeO, Al_2O_3 and SiO_2.

Key: (a) Microns; (b) Melting; (c) Mode.

III. Coupling Loss

In a waveguide gas laser, the mirrors and the waveguide are separated. Therefore, as light radiates into the free space from an opening of the waveguide, light then reenters the waveguide. At that time, there is coupling loss, loss without a complete effective coupling. This coupling loss can be divided into two parts:

1. After departing from the opening of the waveguide, the light field expands. After reflection from the reflective mirror, a part of the light does not enter the opening of the waveguide again.

2. One part of the energy re-entering the opening of the waveguide converts to an high-order mode (that is, not all energy enters the EH_{11} mode).

The problem interesting to the author is how to properly arrange the mirrors in a waveguide laser. By such arrangement, the coupling loss from EH_{11} is minimum. Abrams [9] applied a simplification hypothesis and derived through analysis the relationship between the coupling loss of the EH_{11} mode on one hand, and the radius of curvature R of the mirror and the distance z from the mirror to the opening of the waveguide on the other. The relationship is plotted in Fig. 6. In the figure, b is given by definition as the conjugate foci parameter of the "approximate" gaussian beam.

$$b = \pi w_o^2/\lambda, \qquad (7)$$

Here w_o is the radius of the light beam at the opening of the waveguide with the maximum value of field oscillation amplitude as 1/e value point. $w_o=0.6435a$ [9].

For waveguide lasers with a certain wavelength and aperture diameter a, b is a constant. For example, for λ=10.6 microns, when a=0.75 mm, b=6.9 cm; when a=0.5 mm, b=3.1 cm.

Generally speaking, there are three cavity structures with low coupling loss (<2 percent) for the EH_{11} mode, as follows:

1. For plain mirrors very close to the opening of the waveguide ($z/b<0.1$ and $R/b\to\infty$).

2. For a concave mirror with its center of large radius of curvature approximately at the opening of the waveguide ($z\approx R>8b$).

3. For a concave mirror with its focus at the opening of the waveguide ($z=b$, $R=2b$).

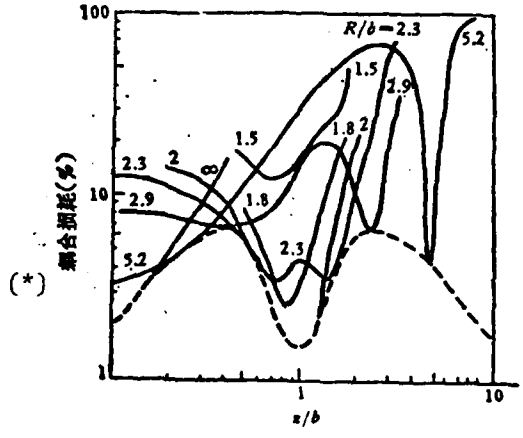

Fig. 6. Relationship between coupling loss of EH_{11} mode and the distance z/b of normalized mirrors.
Key: (*) Coupling loss.

By utilizing the "approximate" gaussian light beam, a qualitative explanation can be made for the above-mentioned low coupling loss cavity structure because the radius of curvature of the local wave front at a distance z from the opening of the waveguide is

$$R' = b(z/b + b/z). \qquad (8)$$

When the mirror surface matches with the wave front which contacts the mirror, the wave front may return to its original shape; therefore, the coupling is effective. In the vicinity of the opening of the waveguide, the wave front is relatively

flat; therefore, a plain mirror has a relatively high coupling efficiency. When z increases, due to its divergence, coupling loss is increased with accompanying

$$L \doteq 57(z/b)^{\frac{1}{2}}\% \quad (z/b \lesssim 0.4). \qquad (9)$$

When z is quite large, the wave front becomes an arc; in this case, by using a concave mirror with appropriate radius of curvature, coupling of very small losses can be obtained.

From the relationship between coupling loss and z in Fig. 6, we can estimate the relationship between z and output power P of the waveguide gas laser, as shown in Fig. 7. For a plain mirror, P simple-harmonically decreases with increasing z. For a concave mirror and $R \leqslant 2b$, a peak value of P will appear with variation of z. However, when $R \geqslant 2b$, two peak values of P will appear with variation of z. Experiments proved the above-mentioned estimates.

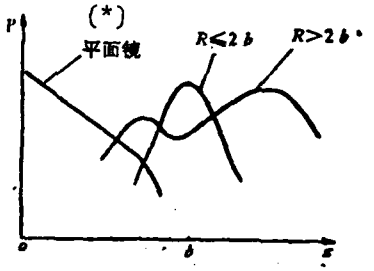

Fig. 7. Relationship between z and output power P.
Key: (*) Plain mirror.

In the three above-mentioned cavity structures, plain mirrors are constantly used. If other elements have to be placed in the cavity, we can use the structure with R=2b and z=b. If there is no limitation on the overall length, very small coupling loss can be obtained in the second type of cavity structure.

IV. Output Power

As with an ordinary CO_2 laser, output power can be calculated by use of the uniform widening equation [10], as the following

$$P = \frac{I_s A \sqrt{r_1} t_2 [g_0 l - \ln (r_1 r_2)^{-\frac{1}{2}}]}{(\sqrt{r_1} + \sqrt{r_2})(1 - \sqrt{r_1 r_2})}, \quad (10)$$

In the equation, A is the area of effective light beam; t_2 is the transmissivity of the output lens; l is the length of discharge; and r_1 and r_2 are reflectivities of the two reflecting mirrors, and for a waveguide gas laser, r_1 and r_2 are the reflectivities of the reflecting mirrors after allowing for deducting waveguide transmission losses and coupling losses [11].

As indicated by equation (10), $P \propto I_s g_0$. As proved by theory and experiments, the saturated light intensity $I_s \propto p^2$; however, the small increment of signal g_0 at the center of spectral lines decreases with increasing gas pressure p. There is the best pressure intensity of gas filled p_{opt}, causing the maximum output power, as shown in Fig. 8.

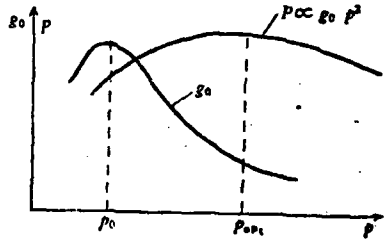

Fig. 8. Principle of relationship between output power and gas-filling pressure intensity.

If all losses of waveguide lasers are neglected, the output power [3, 5] is

$$P = AI_s g_0 l,$$

or

$$P/l = AI_s g_0. \qquad (11)$$

According to the law of equal ratio [3] similar to discharge, in the situation of the best gas filling condition and the best discharge current, g_0 is not related to discharge tube diameter (the waveguide aperture diameter 2a); $I_s \propto \frac{1}{a^2}$. However, $A=\pi a^2$, P/ℓ is not related to a. This means that it is impossible to use a small aperture diameter of the waveguide to raise the output power obtained by a unit length of the waveguide laser. For example, at present we can obtain a maximum of 0.41 watt/cm [5] for a waveguide CO_2 laser. This figure is more or less equal to 40-50 watts per meter as obtained by an ordinary CO_2 laser.

V. Width of Oscillation Belt

In the case of uniform widening, the frequency deflection [11] for a laser to terminate oscillation is

$$|\nu_c - \nu_0| = \frac{\Delta\nu}{2}\left[\frac{g_0 l}{\ln (r_1 r_2)^{-1/2}} - 1\right], \qquad (12)$$

In the equation, ν_c is the frequency at which the oscillation decreases to zero; ν_o is the frequency at the center of the spectral lines; and $\Delta\nu$ is the increasing width of pressure intensity. Therefore, the width of the total oscillation belt is $\Delta\nu_{osc} = 2|\nu_c - \nu_0|$.

As measured from Abrams' [12] experiments, $\Delta\nu$ is proportional to the gas-filling pressure intensity, and is related to mixture ratio and gas temperature. For gas mixing in a typical waveguide CO_2 laser, under working temperatures, the widening ratio is 4.5 megahertz/bar [4].

As indicated by equation (12), $\Delta\nu_{osc} \propto \Delta\nu_{g_0}$. As $\Delta\nu$ increases proportionally with gas-filling pressure intensity p, and g_o decreases with increasing p, there is the best gas-filling pressure intensity p'_{opt} for the maximum width of the oscillation belt. It can be proved [11] that the best gas-filling pressure intensity p'_{opt} to attain the maximum width of the oscillation belt for the waveguide CO_2 laser can also maximize the output power.

Under the best gas-filling condition and the best discharge current situation, g_o is not related to p_{opt}; however, $\Delta\nu$ increases proportionally with p_{opt}. Therefore, $\Delta\nu_{osc}$ also proportionally increases with p_{opt}, that is inversely proportional to the magnitude of the aperture diameter a of the discharge tube.

From the above mentioned, a relatively small aperture diameter a of the discharge tube should be adopted in order to obtain a wide oscillation belt.

Abrams [4] used a waveguide CO_2 laser made of BeO waveguide tube with a=1 mm and ℓ=8.5 cm; the gas-filling pressure intensity is 260 bars, r_1=0.99 and r_2=0.97. From calculation, he derived $\Delta\nu$=1170 megahertz. By using g_o=0.005 $(cm)^{-1}$, Abrams calculated that $2|\nu_c - \nu_0|$ =1285 megahertz. From experiments, at 1.2 kilomegahertz the measurements match the calculation.

According to equation (12), $\Delta\nu_{osc}$ increases with increasing increment length of the waveguide CO_2 laser and decrease of total loss (through r_1 and r_2).

However, in order to have continuous frequency modulation in the entire width of the oscillation band, the increase of ℓ has an upper limit, because there will be a second longitudinal mode oscillation if the cavity length L_c is greater than $c/2\Delta\nu_{osc}$ (c is the speed of light). In order to overcome this limitation by using a greater increment length ℓ, a longitudinal-mode selection technique should be adopted [13].

VI. Structure of Waveguide CO_2 Laser

In a waveguide CO_2 laser, the discharge tube containing gas discharge is also the light waveguide tube. Therefore, the structure of the discharge tube should be considered not only electrically but also optically. Besides, cooling of the working gas in the waveguide CO_2 laser is an important problem [14] because under the best gas-filling condition and the best discharge current situation, the input electric power for a unit length of waveguide tube and the difference between the gas temperature (at the tube axis) and the temperature (on the inner wall) are not related to the discharge tube aperture diameter 2a. However, as a cooling surface, the lateral surface of the waveguide tube decreases proportionally with a. Therefore, the smaller the aperture diameter of the waveguide, the greater is the heat transmitted through a unit cooling surface; thus, the requirements of cooling method and heat conduction property of the waveguide material are higher.

The temperature difference ΔT_w between inner and outer walls of circular and rectangular cross-section waveguide tubes can be, respectively, calculated by using the following equations:

For a circular hole [14],

$$\Delta T_w = \frac{P_{in}}{2\pi l k_w} \ln \frac{R_o}{R_i}, \qquad (13)$$

In the equation, P_{in} is the power produced by discharge in a waveguide tube; ℓ is the length of the waveguide; k_w is the heat conductivity of the waveguide material; and R_o and R_i are outer and inner diameters of the waveguide tube.

For a rectangular hole:

$$\Delta T_w = \frac{bP_{in}}{2a l k_w}, \qquad (14)$$

In the equation, dimensions a and b are shown in Fig. 9.

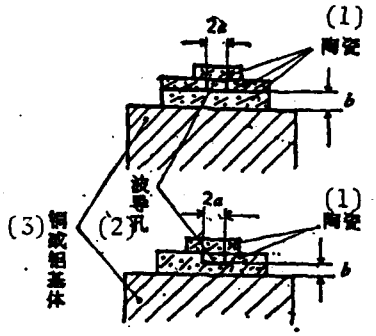

Fig. 9. Cross section of ceramic rectangular-shaped hollow waveguide.
Key: (1) Ceramic; (2) Waveguide hole; (3) Copper or aluminum base.

As indicated by the ΔT_w equation, the higher the heat conductivity of the waveguide material and the thinner the waveguide wall, the smaller is the temperature difference between inner and outer walls of the waveguide. Table 2 lists heat conduction properties of several types of ordinary waveguide materials. Since the value of heat conductivity is related to material purity and its denseness, data in the table are only for reference. However, BeO is the best material from the aspect of a working gas of a cooling waveguide CO_2 laser.

Table 2. Heat conduction properties of common materials.

(1) 材料	(2) 热导率(卡/厘米·秒·度)
BeO	5.24×10^{-1}
BN	$\sim1\times10^{-1}$
Al_2O_3	5.4×10^{-2}

Key: (1) Materials; (2) Heat conductivity (calorie/cm·sec·degree).

No matter what the aspect of waveguide transmission loss, or the aspect of cooling of discharge tube, the smaller the aperture diameter of a waveguide CO_2 laser, the greater the need to use BeO ceramic as the material of the waveguide medium. Since it is required to have a very wide oscillation belt (of a waveguide CO_2 laser), the aperture diameter of the discharge tube should be very small. Therefore, in this type of waveguide CO_2 laser, BeO should be used as waveguide notwithstanding shortcomings (of BeO) in terms of toxicity, brittleness and less compactness. However, for a waveguide CO_2 laser not requiring a very wide oscillation belt, the aperture diameter of the waveguide can (and should) be made larger. Thus, Al_2O_3 or ordinary boron-silicate glass type materials can be used to make the waveguide tube.

In the following, several structures are reported.

Figure 10 shows an easily-made glass waveguide CO_2 laser [16] used in experiments. Both terminals of the discharge tube are processed with acetal resin to compose a dismantlable structure. In addition, an O-type sealing ring is used for assembly into the laser tube. Therefore, this structure is convenient to interchange and remodel.

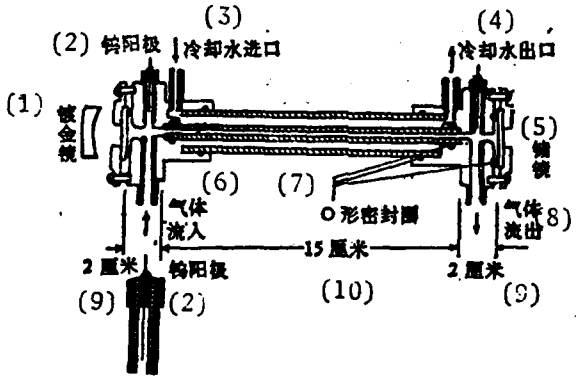

Fig. 10. Assembled-type glass waveguide CO_2 laser.
Key: (1) Gold-coated mirror; (2) Tungsten anode; (3) Inlet of cooling water; (4) Outlet of cooling water; (5) Germanium lens; (6) Gas inflow; (7) O-shaped sealing ring; (8) Gas outflow; (9) 2 cm; (10) 15 cm.

Figure 11 also shows a waveguide CO_2 laser [17] made of glass. The laser adopts dual discharge, and NaCl is used as the window plate of the discharge tube. The optical resonance oscillation cavity is composed of a diffraction light grating (with 150 lines per millimeter) and a gold-coated concave lens which is fixed on piezo-ceramic. By rotating the light grating, laser skip can be selected. The oscillation frequency in increment lines is adjusted by slightly changing the cavity length through the piezoelectric ceramic. At L=26.5 cm, it was observed that the modulation range was over 570 megahertz. When a plain lens is used to substitute the concave lens, the cavity length L_c can be shortened to 21.5 cm and the modulation range can exceed 700 megahertz.

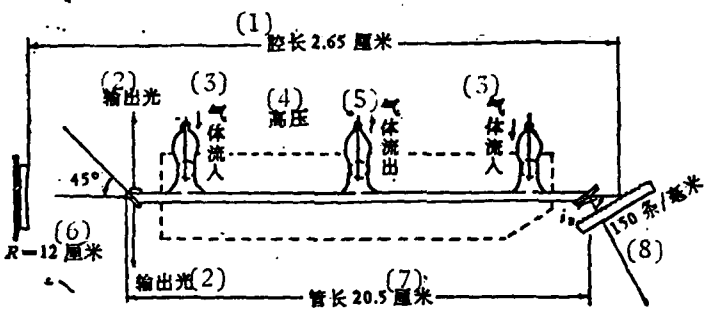

Fig. 11. Glass waveguide CO_2 laser with modulable frequency. Key: (1) Cavity length at 2.65 cm; (2) Output light; (3) Gas inflow; (4) High pressure; (5) Gas outflow; (6) R=12 cm; (7) Tube length at 20.5 cm; (8) 150 lines per millimeter.

Figure 12 shows a square waveguide CO_2 laser [3] composed of two stepped and polished Al_2O_3 plates of ceramic. Three holes were opened in one of the Al_2O_3 ceramic plates; the middle hole sealed with a metal tube is used as cathode and exhuast gas tube. At two sides, the two holes sealed with needle-shaped electrodes are used as anode.

The structure [13] shown in Fig. 13 used a 99.5 percent purity BeO rod (12.9 cm) to drill a 2.25-cm diameter hole as the waveguide tube. Cooling of the laser uses insulated flowing fluorocarbon liquid. This laser produces the highest unit length output at 410 milliwatts per centimeter. The use of invar shell and

piezoelectric ceramic can lead to modulable output with steady frequency. Adjustment of the angle of the reflective mirror utilizes the easy deformability of invar with four adjusting screws.

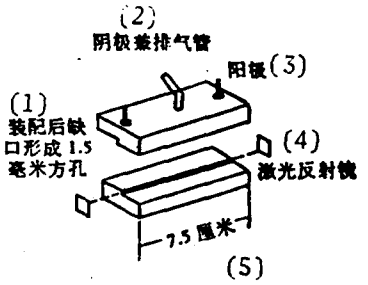

Fig. 12. Al_2O_3 ceramic square waveguide CO_2 laser.
Key: (1) After assembly, the gap is a square hole with 1.5 mm sides; (2) Cathode and exhaust gas tube; (3) Cathode; (4) Laser reflective mirror; (5) 7.5 cm.

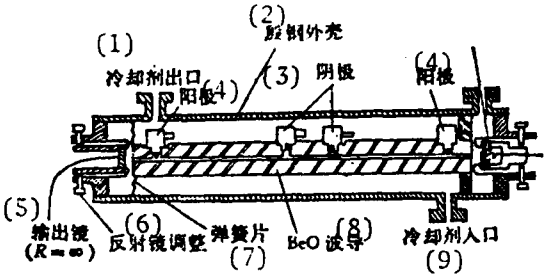

Fig. 13. BeO circular waveguide CO_2 laser with adjustable frequency.
Key: (1) Exit of cooling agent; (2) Invar shell; (3) Anode; (4) Cathode; (5) Output lens; (6) Adjustment of reflective mirror; (7) Spring plate; (8) BeO waveguide; (9) Inlet of cooling agent.

The structure shown in Fig. 14 is an 1-mm square waveguide composed of four plates of BeO [4]; the working gas in the waveguide is cooled with a BeO ceramic plate using a water-cooling type heat sink. The output of the laser is coupled out from zero-level reflection of an 150-line-per-millimeter diffraction light grating. The function of the selector of the initial spectral lines of the light grating causes oscillation in the linear polarized mode.

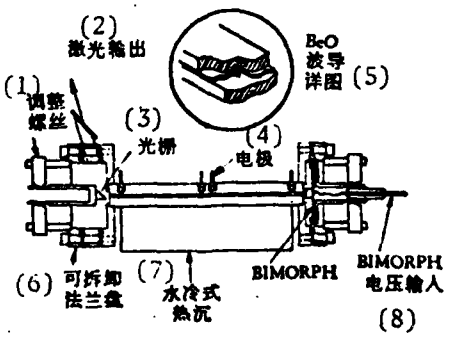

Fig. 14. BeO square waveguide CO_2 laser with adjustable frequency.

Key [of Fig. 14 on the preceding page]: (1) Adjusting screw; (2) Laser output; (3) Light grating; (4) Electrode; (5) Detailed diagram of BeO waveguide; (6) Dismantlable flange; (7) Water cooling type heat sink; (8) Input of BIMORPH voltage.

LITERATURE

[1] P. W. Smith, *Appl. Phys. Lett.*, 19-5(1971), 132—134.
[2] J. J. Degnan, *Appl. Phys.*, 12(1976), 26.
[3] R. L. Abrams, *IEEE J. Quant. Electr.*, QE-9 (1973), 940.
[4] R. L. Abrams, *Appl. Phys. Lett.*, 25(1974), 304.
[5] D. R. Hall, *J. Phys. D: Appl. Phys.*, 10(1977), 1—6.
[6] D. R. Hall, *J. Appl. Phys.*, 48-3(1977), 1212
[7] E. A. J. Marcatili, *B. S. T. J.*, 43(1964), 1783.
[8] D. Marcuse, Theory of Dielectric Optical Waveguides, New York, 1974.
[9] R. L. Abrams, *IEEE J. Quant. Electr.*, QE-8 (1972), 838.
[10] W. W. Rigrod, *J. Appl. Phys.*, 36(1965), 2487.
[11] J. J. Degnan, *J. Appl. Phys.*, 45(1974), 257.
[12] R. L. Abrams, *Appl. Phys. Lett.*, 25(1974), 609.
[13] W. R. Leeb, *Appl. Opt.*, 14(1975), 1706.
[14] H. Shilds, *J. Appl. Phys.*, 48-11(1977), 4807—4808.
[15] A. Papayoanou, *IEEE J. Quant. Electr.*, QE-13 (1977), 27—29.

[16] Matsumura, et al., Quarterly of Electric Wave Research Institute, (1976), 151-162.

[17] Lyszyk, M. et al., J. Phys. E: Scientific Instruments, 10-11 (1977), 1110-1112.

DISTRIBUTION LIST

DISTRIBUTION DIRECT TO RECIPIENT

ORGANIZATION	MICROFICHE
A205 DMAHTC	1
A210 DMAAC	1
B344 DIA/RTS-2C	9
C043 USAMIIA	1
C500 TRADOC	1
C509 BALLISTIC RES LAB	1
C510 R&T LABS/AVRADCOM	1
C513 ARRADCOM	1
C535 AVRADCOM/TSARCOM	1
C539 TRASANA	1
C591 FSTC	4
C619 MIA REDSTONE	1
D008 NISC	1
E053 HQ USAF/INET	1
E403 AFSC/INA	1
E404 AEDC/DOF	1
E408 AFWL	1
E410 AD/IND	1
E429 SD/IND	1
P005 DOE/ISA/DDI	1
P050 CIA/OCR/ADD/SD	2
AFIT/LDE	1
FTD	
CCN	1
NIA/PHS	1
NIIS	2
LLNL/Code L-389	1
NASA/NST-44	1
NSA/1213/TDL	2